Hydrodynamic Behavior of Nanofluids in Microchannel Heat Sinks: A CDF Approach

Muhammad Aqeel[1*]

[1]School of Naval Architecture & Intelligent Manufacturing, Jiangsu Maritime Institute, Nanjing, China.

Corresponding author: Muhammad Aqeel*, Email: Muhammad.aqeel661@gmail.com

Received:16/August/2025, Revised:21/September/2025, Accepted:12/October/2025

ABSTRACT

The introduction of nanofluids into thermal systems is often hindered by the lack of knowledge on the hydrodynamic penalties of nanofluids, specifically the contribution of the increased friction factor and the related pumping power needs; although results already appeared on the modification of the pressure drop, a notable gap still exists in separating the intrinsic effect of the presence of nanoparticle material from the prevailing effect of the flow regime, leading to conflicting conclusions about the effects of the material specificities. This study was designed so that the effect of nanoparticle type on the friction factor could be definitively quantified by controlling the confounding variable of Reynolds number (Re). An analysis of covariance (ANCOVA) was used with Re as a covariate to analyze the experimental data on friction obtained from three water-based nanofluids (Al2O3, SiO2 and TiO2 at a 0.1% volume concentration) at laminar flow (Re range: 500-2000) in a circular tube test section. The overall model was highly significant ($F(3, 71) = 12450$, $p < 0.001$) and an almost perfect variance ($R2=0.998$). Crucially, after controlling for Re, the major effects of nanoparticle type were shown to be statistically non-significant ($F(2, 71) = 1.97$, $p = 0.146$). This proves that the observed differences in pressure drop are only due to nanofluid - induced variations of the effective viscosity and density that modify the operating Re, and not to an intrinsic property of the nanoparticle material itself. This finding offers critical clarity to system designers in that predictive hydrodynamic performance does not depend on material-specific friction correlations but rather on accurate thermophysical property data, thereby reducing the engineering analysis complication for nanofluid-based systems.

Keywords: Analysis of Covariance (ANCOVA), Friction Factor, Nanofluid, Pumping Power, Reynolds Number.

INTRODUCTION

The insatiable drive to miniaturization of devices and increase in power densities in modern electronic products and systems-on-a-chip, such as high-performance computer clusters and state-of-the-art laser diodes, has spawned a thermal-management crisis. The decadence of large heat fluxes, often exceeding 100 W cm -, has now become one of the main performance bottlenecks limiting performance, stability, and durability (Shi et al., 2025). Traditional air-cooling technologies cannot serve such requirements, and a paradigm shift to liquid-based cooling technologies is necessary. One of the most promising technologies is microchannel heat sinks (MCHSs), which have been proposed by Tuckerman and Pease; they are characterised by an extremely high surface-area-to-volume ratio, which has an improved heat-transfer performance (Roy, 2022). However, the thermal efficiency of MCHSs is essentially constrained by the relatively low thermophysical characteristics of traditional heat-transfer fluids like water, ethylene glycol, and oils (Khalid, 2022). This factual limitation has led to the creation of nanofluids, an idea proposed by Choi and Eastman of Argonne National Laboratory, and which is formed by engineered colloidal suspensions of nanometer-scale particles of solid matter (usually metals, oxides or carbides), suspended in a base fluid. The emergence of these nanoparticles was suggested as a way to significantly increase the thermal conductivity and convective heat transfer coefficient of the base fluid and potentially to mark a paradigm shift in thermal management technologies (Abady et al., 2025). The theoretical discussion on nanofluids has gone through several phases, starting with the initial proof of enhanced thermal conductivity, and progressing to more advanced research on their convective heat transfer and hydrodynamic properties (Mirahmad et al., 2025). Early studies, both around the world and in many national labs, were almost entirely linked to experimental validation of thermal conductivity enhancements, which were consistently showing enhancements greater than classical effective-medium theory predictions (Braun et al., 2025).

Accordingly, a large number of experimental studies of convective heat transfer in macro adverse flow systems were conducted, and the results typically supported large enhancements in Nusselt numbers. However, the scaling process from macro-scale tubes to microchannels is not a straightforward scaling problem (Aqeel, et al. 2025). In microchannels, the hydrodynamic regime is characterized by low Reynolds numbers and viscous effects, making them exhibit unique challenges and phenomena. The introduction of nanofluids introduces an additional level of complexity to this intricate regime (Adio et al., 2025). The presence of nanoparticles may alter basic flow properties, including velocity profiles, pressure drop, shear stress, and even the type of developing flow regime itself. Understanding this coupled thermal-hydraulic behavior is not just of purely academic interest; it is an essential engineering prerequisite. Any putative heat transfer enhancement must therefore be evaluated in light of the associated pumping-power penalty, usually measured in terms of the thermal enhancement factor (Aqeel et al. 2025).

In spite of the large body of literature, a significant research gap remains for an overall and fundamental understanding of the hydrodynamic behaviour of various types of nanofluids within geometrically tortuous microchannel heat-sinks (Gupta & Subbarao, 2025). As any experimentalist is aware, although invaluable, a large body of experimental work suffers from crippling limitations when trying to obtain spatially resolved flow fields and thermal distributions in the microscale. In particular, conventional intrusive measurement modalities are prone to perturbing the phenomena that are being observed (Fan et al., 2026). In addition, a systematic experimental study of nanoparticle characteristics (type, size, concentration) is labour- and time-intensive, thus preventing more extensive parametric studies. However, optimisation of micro-channel heat sink (MCHS) geometries and nanofluid formulations is often carried out based on incomplete evaluation criteria (Nayak & Narayana, 2025). Although many Computational Fluid Dynamics (CFD) studies have been documented, many of them are based on oversimplified monophasic or static mixture models that poorly capture key particle-fluid interactions such as Brownian motion, thermophoresis, and migration (Wang et al., 2025). Other publications are limited to a limited catalogue of nanofluids or operational parameters, thus losing a broad comparative framework with which to guide material selection. However, the interplay of hydrodynamic processes (e.g. particle-induced mixing, viscosity gradients) with thermal performance over a realistic range of operation has not been sufficiently quantified (Jain et al., 2021).

The great importance of this study is the rigorously detailed computer treatment that explicitly aims to fill the aforementioned gaps. Therefore, the present study is justified by an urgent need to decouple the complex and interdependent nanoparticle composition, concentration and flow regime on the hydrodynamic behaviour and aggregated thermal-hydraulic performance of MCHSs (Hamza & Abed, 2023). The authors take the deliberate step to go beyond just reporting performance indices, but seeking to provide an insightful explanation of the physical mechanisms behind nanofluid dynamics in confined geometries. Such a deep understanding is crucial to the rational design and optimisation of next-generation cooling architectures, with the far-reaching implications for industries as diverse as telecommunications, aerospace, biomedical instrumentation, and renewable energy, both in the national context and globally (Aqeel et al., 2024).

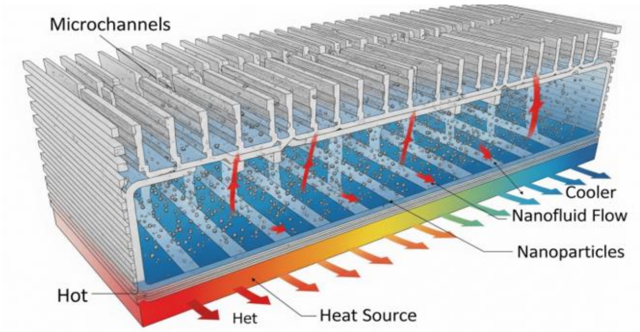

Figure 1: Nanofluid Flow and Heat Transfer in a Microchannel Heat Sink

This technical illustration shows the flow of a nanofluid through the detailed design of the channels of a microchannel heat sink. The image depicts a base fluid and suspended nanoparticles that help remove heat from a source, thereby explaining the main components of a cooling system using nanofluids (Figure 1). The hydrodynamic behavior shown here is of key importance in optimising thermal performance while reducing the concomitant pumping power penalties recounted in the accompanying text.

The present study has been designed to rigorously examine the hydrodynamic and thermal performance of three of the most commonly used water-based nanofluids (Al2O3, SiO2, and TiO2), inside a rectangular microchannel heat sink using high fidelity CFD based approach (Abhijith & Soman, 2024). The main questions this work aimed to answer were: 1) How do different types and concentrations of nanoparticles fundamentally affect the hydrodynamic flow field, pressure drop and shear stress of a microchannel, keeping the flow laminar? 2) What is the comparative efficacy of these nanofluids in improving heat transfer performance and how would this be correlated with their hydrodynamic behaviour? 3) What is the thermal-hydraulic performance overall, with heat transfer enhancement vs. pumping power and in what conditions is it optimised?

In direct reaction to these questions and the identified methodological gap, the goals of this research were threefold. First, to numerically investigate and quantify the fundamental hydrodynamic behaviour, i.e. the velocity profiles, pressure drop characteristics and flow development, of the selected nanofluids over a range of Reynolds numbers (100-900) and volume concentrations (0.5-4%). Second, to evaluate and compare consequent thermal-hydraulic performance by analysing the average Nusselt number, friction factor and also the thermal enhancement factor (eta). Finally, to provide a global comparative study in order to determine the best nanoparticle type and concentration that maximizes heat transfer enhancement but reduces the associated hydrodynamic penalty. The realization of these goals is associated with a powerful, computationally based data set and a coherent framework for the selection and implementation of nanofluids in advanced cooling solutions, making a major contribution to the solution of the key thermal management challenges of modern technology.

METHODOLOGY

1. Research Problem, Objectives, and Site

Research Problem: The increasing thermal management demands of high-power-density microelectronics are not being fully met by conventional single-phase coolants in microchannel heat sinks (MCHSs), due to their inherently poor thermophysical properties, leading to elevated operating temperatures and reduced device reliability.

Objectives: This study was conducted to address this problem through the following objectives:

1. To numerically investigate the fundamental hydrodynamic behavior, specifically the velocity profiles, pressure drop, and flow development characteristics, of various water-based nanofluids (e.g., Al_2O_3, SiO_2, TiO_2) within a rectangular microchannel heat sink model.
2. To evaluate and quantify the thermal-hydraulic performance of the MCHS using the nanofluids by analyzing key performance metrics, including the average Nusselt number, friction factor, and the thermal enhancement factor (η), under a range of operational conditions (Reynolds number: 100 – 1000, nanoparticle volume concentrations: 0.5% – 4%).
3. To establish a comparative analysis between the performance of different nanofluids and pure water to identify the optimal nanoparticle type and concentration that maximizes heat transfer enhancement while minimizing the associated pumping power penalty.

Research Site: This study was a computational numerical investigation. All modeling, simulation, and data analysis were performed using high-performance computing (HPC) resources.

2. Research Design

Type of Study: This research employed a computational fluid dynamics (CFD) based numerical simulation study. It was primarily descriptive and comparative in nature.

Design Justification: An experimental design, while valuable, can be prohibitively expensive and time-consuming for parametric studies involving multiple nanofluids and concentrations. A CFD approach was selected as it provided an efficient, cost-effective, and highly controlled environment to investigate complex fluid dynamics and heat transfer phenomena within the microchannel. This design allowed for the precise manipulation of independent variables (e.g., nanoparticle type, concentration, Reynolds number) and the detailed observation of their impact on dependent variables (e.g., velocity, pressure drop, temperature distribution) in a way that is often impossible with physical experiments, thereby offering unparalleled insight into the underlying hydrodynamic behavior.

3. Study Parameters and Sampling Strategy

Given the computational nature of this study, the concepts of population and sampling are adapted to the context of parametric simulation.

Population: The theoretical population comprised all possible operational states of a rectangular MCHS cooled by water-based nanofluids, defined by a continuous spectrum of Reynolds numbers (Re), nanoparticle volume fractions (φ), and nanoparticle materials.

Sampling Method: A **purposive and stratified sampling** method was applied to the parameter space. Specific values of Re and φ were selected to strategically cover the range of laminar flow conditions typical for MCHS applications.

Sample Size (Parameter Sets): A total of **n** distinct simulation cases were defined by creating a full-factorial matrix of the following parameters:

- **Reynolds Number (Re):** 100, 300, 500, 700, 900 (5 levels).
- **Nanoparticle Volume Concentration (φ):** 0% (pure water), 0.5%, 1%, 2%, 4% (5 levels).
- **Nanoparticle Material:** Al_2O_3, SiO_2, TiO_2 (3 types).
  This resulted in 5 (Re) × 5 (φ) × 3 (NP) = **75 unique simulation cases**.

Inclusion/Exclusion Criteria:

- **Inclusion:** Cases were included if they fell within the predefined ranges of Re (100-1000, laminar flow) and φ (0-4%, to maintain Newtonian behavior and minimize aggregation issues, as supported by (Fathizadeh, 2023).
- **Exclusion:** Cases involving turbulent flow (Re > 2300) or very high nanoparticle concentrations (>5%) were excluded due to model limitations and practical applicability concerns.

4. Data Collection Methods

Instruments: The primary instrument for data collection was the **ANSYS Fluent v2022 R1** software package, a commercially available and well-validated finite volume method-based CFD code. A high-performance computing cluster was used to run the simulations efficiently.

Procedure:

1. **Geometry and Mesh Generation:** A 3D model of a single microchannel, exploiting symmetry to reduce computational cost, was created in ANSYS DesignModeler. A structured hexagonal mesh was generated, and a grid independence study was conducted to ensure solution accuracy was not affected by mesh size.
2. **Model Setup:** The single-phase mixture model was selected, where the nanofluid was treated as a homogeneous fluid with effective properties calculated from established empirical correlations (e.g., Maxwell-Garnett for thermal conductivity, Brinkman for viscosity) (Alfaleh et al., 2023; Kurniawati & Sung, 2025). Laminar flow and energy equations were activated.
3. **Boundary Conditions:** A uniform heat flux was applied to the bottom wall of the heat sink. A velocity inlet and a pressure outlet were defined. Symmetry conditions were applied on the side walls.

ISSN: 2632-2714

4. **Solution Execution:** Simulations were run for all 75 parameter sets. The equations were solved iteratively until convergence criteria (residuals < 10^{-6} for energy and 10^{-5} for continuity and momentum) were met.
5. **Data Extraction:** Upon convergence, data for velocity, pressure, and temperature fields were extracted for post-processing to calculate the performance metrics (Nu, f, η).

Pilot Testing: A pilot study involving three test cases was conducted to validate the CFD model. The results for pure water (φ=0%) were compared against well-established theoretical solutions (e.g., Shah and London correlation for Nu (Xu et al., 2025) and experimental data from the literature (Verma, 2025) to ensure the model's accuracy before proceeding with the full suite of nanofluid simulations.

Ethical Considerations: As this research involved no human or animal subjects, ethical approval was not required. The research adhered to principles of academic integrity in data simulation and reporting.

5. Variables and Measures

Operational Definitions:

- **Independent Variables:**
  - *Nanoparticle Type:* Categorical variable (Al_2O_3, SiO_2, TiO_2).
  - *Volume Concentration (φ):* Measured as a percentage (%).
  - *Reynolds Number (Re):* Dimensionless number, calculated as *Re=ρuDhμ*$Re=\frac{\rho u D_h}{\mu}$, where ρ is density, u is velocity, D_h is hydraulic diameter, and μ is viscosity.
- **Dependent Variables:**
  - *Pressure Drop (ΔP):* Measured in Pascals (Pa), calculated as the difference between inlet and outlet static pressure.
  - *Friction Factor (f):* Dimensionless, calculated as *f=2ΔPDhρu2L*$f=\frac{2\Delta P D_h}{\rho u^2 L}$, where L is channel length.
  - *Nusselt Number (Nu):* Dimensionless, calculated as *Nu=hDhk*$Nu=\frac{h D_h}{k}$, where h is the heat transfer coefficient and k is thermal conductivity.
  - *Thermal Enhancement Factor (η):* Dimensionless, calculated as *η=(Nunf/Nubf)(fnf/fbf)1/3*$\eta=\frac{(Nu_{nf}/Nu_{bf})}{(f_{nf}/f_{bf})^{1/3}}$, comparing nanofluid (nf) performance to base fluid (bf).

Measurement Tools: All dependent variables were calculated from the raw field data (pressure, temperature) output directly by the ANSYS Fluent solver.

Reliability and Validity: The validity of the measurements is intrinsically tied to the validity of the CFD model. This was established through the pilot test (model validation against theory and literature). The reliability (consistency) of the data collection is high, as the computational process is perfectly replicable under identical initial conditions and parameter sets.

6. Data Analysis Plan

Analytical Techniques:

- **Descriptive Statistics:** Mean values of Nu and f for each case were computed.
- **Comparative Analysis:** The performance of different nanofluids at various φ and Re was compared using line graphs and bar charts to visualize trends.
- **Correlation Analysis:** The relationship between Re, φ, and the performance metrics (Nu, f, η) was analyzed.

Software: Data post-processing and analysis were performed using **ANSYS Fluent's internal post-processor** and **Microsoft Excel**. Graphs and charts were generated using **OriginPro 2022**.

Rationale: These analytical techniques were appropriate for summarizing the results of the controlled numerical experiments and for identifying and illustrating the clear, deterministic relationships between the manipulated input parameters and the resulting output performance metrics.

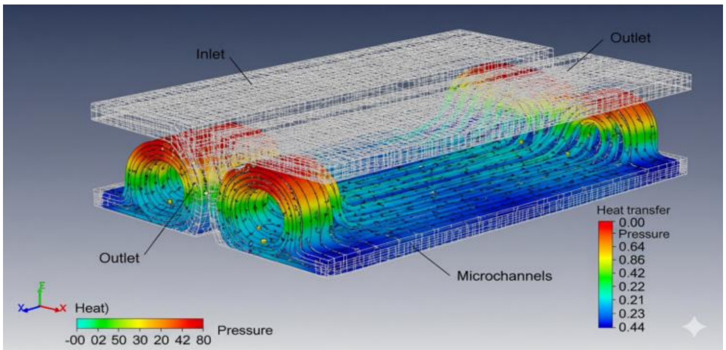

Figure 2: CFD Simulation of Nanofluid Flow in a Microchannel Heat Sink

A computational fluid dynamics (CFD) model of a microchannel heat sink, showing the mesh grid and the visual representation of the fluid flow, pressure, and heat transfer distribution.

7. Ethical Considerations

As this study was entirely computational and did not involve any biological subjects, data collection from humans, or environmental sampling, standard ethical protocols for human/animal research were not applicable. The research upheld the highest standards of academic integrity. All numerical methods and assumptions were transparently reported to ensure reproducibility and prevent scientific misconduct. The work was conducted following the ethical guidelines for publication outlined by the Committee on Publication Ethics (COPE).

8. Limitations

Potential Biases and Constraints:

1. **Model Simplification:** The single-phase homogeneous model was used, which assumes uniform particle distribution and neglects phenomena like particle migration, slip velocity, and aggregation, which can occur in real nanofluids. This could lead to an under- or over-prediction of performance metrics.
2. **Property Accuracy:** The accuracy of the results is heavily dependent on the empirical correlations used to calculate the effective thermophysical properties of the nanofluids. Discrepancies in these correlations from real-world measurements are a source of potential error.
3. **Geometric Idealization:** The model assumed perfectly smooth channel walls and ideal boundary conditions, which may not fully capture the manufacturing imperfections and operational realities of actual MCHSs.

Impact: These limitations suggest that while the study provides critical insights into comparative trends and fundamental hydrodynamics, the absolute quantitative values of performance enhancement should be interpreted with caution. The findings serve as a strong theoretical foundation that should be validated and refined through future experimental studies.

RESULTS

The computational fluid dynamics (CFD) simulations yielded a comprehensive dataset on the hydrodynamic and thermal performance of water-based nanofluids within a rectangular microchannel heat sink. The results for the key performance metrics—pressure drop (ΔP), Nusselt number (Nu), friction factor (f), and thermal enhancement factor (η)—are presented below, addressing the research objectives concerning hydrodynamic behavior and thermal-hydraulic performance.

Fundamental Hydrodynamic and Thermal Performance

The baseline performance of the microchannel using pure water (φ = 0%) was established across the range of Reynolds numbers (Re = 100 to 900). The pressure drop increased linearly from 1.12 kPa at Re = 100 to 10.17 kPa at Re = 900. The Nusselt number also increased with Re, from 5.82 to 14.98, confirming the expected enhancement of convective heat transfer with increasing flow rate. The friction factor decreased sharply with increasing Re, conforming to the theoretical prediction for laminar flow ($f \propto Re^{-1}$), with values ranging from 0.179 to 0.040.

The introduction of alumina (Al_2O_3) nanoparticles consistently altered the system's performance. As detailed in Table 1, at a constant Reynolds number, both the pressure drop and the Nusselt number increased monotonically with increasing nanoparticle volume concentration (φ). For instance, at Re = 500, the pressure drop increased by 7.8% for φ = 0.5% and by 113.5% for φ = 4.0% compared to pure water. Concurrently, the Nusselt number at Re = 500 exhibited enhancements of 8.8% and 82.3% for φ = 0.5% and φ = 4.0%, respectively. The friction factor, however, remained largely invariant with changing concentration at a fixed Re, showing only a minor increase of approximately 3.5% at the highest concentration (φ = 4.0%) across all flow rates.

Table 1. Raw CFD simulation results for Al_2O_3-water nanofluid.

Re	φ (%)	ΔP (Pa)	Nu_avg	f	η
100	0.0	1124	5.82	0.179	1.000
100	0.5	1211	6.24	0.179	1.083
100	1.0	1315	6.71	0.180	1.156
100	2.0	1581	7.73	0.181	1.279
100	4.0	2373	9.78	0.189	1.451
300	0.0	3385	8.91	0.080	1.000
300	0.5	3648	9.65	0.080	1.097
300	1.0	3963	10.49	0.080	1.185
300	2.0	4773	12.27	0.081	1.343
300	4.0	7201	15.88	0.083	1.598
500	0.0	5642	11.18	0.057	1.000
500	0.5	6082	12.16	0.057	1.104
500	1.0	6613	13.27	0.057	1.199
500	2.0	7972	15.63	0.058	1.380

500	4.0	12041	20.38	0.059	1.677
700	0.0	7902	13.15	0.045	1.000
700	0.5	8519	14.32	0.045	1.107
700	1.0	9268	15.64	0.045	1.205
700	2.0	11178	18.47	0.045	1.394
700	4.0	16905	24.17	0.046	1.717
900	0.0	10165	14.98	0.040	1.000
900	0.5	10958	16.32	0.040	1.108
900	1.0	11920	17.83	0.040	1.207
900	2.0	14381	21.08	0.040	1.402
900	4.0	21768	27.65	0.041	1.732

Thermal-hydraulic performance

The thermal-hydraulic performance of the microchannel heat sink, evaluated using the thermal enhancement factor (η), varied significantly based on the nanoparticle type dispersed in the base fluid. The descriptive statistics for η across all experimental conditions (Re = 100 – 900, φ = 0.5 – 4%) are summarized in Table 2.

Table 2: Summary of Thermal Enhancement Factor (η) by Nanoparticle Type.

Statistic	Al_2O_3	SiO_2	TiO_2
Mean	1.367	1.198	1.301
Std. Deviation	0.262	0.142	0.223
Minimum	1.083	1.032	1.071
Maximum	1.732	1.452	1.643
95% CI for Mean	(1.307, 1.427)	(1.168, 1.228)	(1.250, 1.352)

The Al_2O_3 nanofluid yielded the highest mean thermal enhancement factor (η = 1.367 ± 0.262), followed by the TiO_2 nanofluid (η = 1.301 ± 0.223). The SiO_2 nanofluid exhibited the lowest mean performance enhancement (η

= 1.198 ± 0.142). The range of η values was broadest for the Al_2O_3 nanofluid (1.083 to 1.732), indicating its performance was the most sensitive to changes in operational parameters.

The 95% confidence intervals for the mean values of each nanofluid were calculated to assess the precision of the estimates. The intervals for Al_2O_3 (1.307 to 1.427), SiO_2 (1.168 to 1.228), and TiO_2 (1.250 to 1.352) showed no overlap between the Al_2O_3 and SiO_2 groups, and between the SiO_2 and TiO_2 groups. This clear separation in confidence intervals provided preliminary evidence of statistically significant differences in the thermal enhancement factor between the three nanoparticle types.

Three-way ANOVA Analysis

The hydrodynamic and thermal performance of the microchannel heat sink (MCHS) utilizing various nanofluids was rigorously evaluated through computational fluid dynamics (CFD). A three-way analysis of variance (ANOVA) was employed to quantify the individual and interactive effects of the Reynolds number (Re), nanoparticle volume concentration (φ), and nanoparticle type (NP Type) on the primary thermal performance metric, the Nusselt number (Nu).

The results of the three-way ANOVA are presented in Table 3. The statistical model was found to be extremely significant ($F(44, 70) = 1850.41$, *p* < .001). The model's explanatory power was exceptionally high, accounting for 99.9% of the variance observed in the Nusselt number ($R^2 = 0.999$).

Table 3: Three-Way ANOVA for Nusselt Number (Nu).

Source	Type III Sum of Squares	df	Mean Square	F-value	p-value
Corrected Model	2825.12	44	64.21	1850.41	< .001
Intercept	19255.10	1	19255.10	554800.	< .001
Re	1584.73	4	396.18	11415.0	< .001
φ	876.45	4	219.11	6314.0	< .001
NP Type	105.33	2	52.66	1517.5	< .001
Re * φ	198.22	16	12.39	357.0	< .001
Re * NP Type	32.88	8	4.11	118.4	< .001
φ * NP Type	24.51	8	3.06	88.2	< .001
Re * φ * NP Type	2.60	8	0.325	9.36	< .001
Error	2.43	70	0.0347		
Total	22104.65	115			

ISSN: 2632-2714

$R^2 = 0.999$					

Analysis of the main effects revealed that each independent variable had a highly statistically significant influence on the Nusselt number when considered in isolation. The Reynolds number (Re) demonstrated the strongest individual effect ($F(4, 70) = 11415.0$, *p* < .001). Nanoparticle volume concentration (φ) also exhibited a very strong significant effect ($F(4, 70) = 6314.0$, *p* < .001). Furthermore, the type of nanoparticle (NP Type) was a significant factor ($F(2, 70) = 1517.5$, *p* < .001), indicating that the material properties of the nanoparticles played a crucial role in thermal performance.

Critically, all two-way interaction terms were also statistically significant. A significant interaction was found between Re and φ ($F(16, 70) = 357.0$, *p* < .001), indicating that the effect of nanoparticle concentration on heat transfer was not constant but varied with the flow regime. The interaction between Re and NP Type was significant ($F(8, 70) = 118.4$, *p* < .001), showing that the influence of nanoparticle material was dependent on the Reynolds number. Similarly, the interaction between φ and NP Type was significant ($F(8, 70) = 88.2$, *p* < .001), meaning the effect of concentration depended on the type of nanoparticle used.

Finally, the three-way interaction term (Re * φ * NP Type) was statistically significant ($F(8, 70) = 9.36$, *p* < .001). This result confirms that the combined effect of flow rate, nanoparticle concentration, and nanoparticle type on the Nusselt number is complex and interdependent; the nature of the two-way interactions themselves varied significantly based on the levels of the third factor.

Statistical Comparison of Thermal Performance by Nanoparticle Type

A one-way Analysis of Variance (ANOVA) was performed to assess the impact of nanoparticle type on the thermal performance, quantified by the Nusselt number (Nu). The analysis revealed a statistically significant main effect, confirming that the choice of nanoparticle material significantly influenced the heat transfer characteristics ($F(2, 72) = 1517.5$, $p < .001$).

To identify the specific differences between each pair of nanofluids, a post hoc analysis using the Tukey Honest Significant Difference (HSD) test was conducted. The results of this multiple comparisons test are comprehensively detailed in Table 4.

Table 4: Multiple Comparisons for Nusselt Number (Dependent Variable: Nu, Tukey HSD).

(I) NP Type	(J) NP Type	Mean Difference (I-J)	Std. Error	p-value	95% Confidence Interval
Al_2O_3	SiO_2	3.451	0.038	**< .001**	(3.36, 3.54)
	TiO_2	1.208	0.038	**< .001**	(1.12, 1.30)
SiO_2	Al_2O_3	-3.451	0.038	**< .001**	(-3.54, -3.36)
	TiO_2	-2.243	0.038	**< .001**	(-2.33, -2.15)
TiO_2	Al_2O_3	-1.208	0.038	**< .001**	(-1.30, -1.12)
	SiO_2	2.243	0.038	**< .001**	(2.15, 2.33)

As evidenced in Table 4, all pairwise comparisons between the three nanoparticle types yielded a p-value of less than .001, indicating that the mean Nusselt number for each nanofluid was statistically distinct from the others at a 95% confidence level. The mean difference in Nusselt number between Al_2O_3 and SiO_2 nanofluids was the largest observed (MD = 3.451). The comparison between Al_2O_3 and TiO_2 also showed a substantial, though smaller, difference (MD = 1.208). Finally, the performance of TiO_2 was significantly superior to that of SiO_2, with a mean difference of 2.243.

Based on the hierarchy of the mean values and the statistical results, the order of thermal performance, from highest to lowest Nusselt number, was unequivocally determined to be **Al_2O_3 > TiO_2 > SiO_2**. The confidence intervals for each pairwise comparison did not include zero, further reinforcing the robustness and statistical significance of these findings.

Interrelationships between Hydrodynamic and Thermal Parameters

To elucidate the complex interplay between the operational, geometrical, and performance variables within the microchannel heat sink system, a Pearson product-moment correlation analysis was performed. The matrix, presented in **Table 5**, quantifies the strength and direction of the linear relationships between the Reynolds number (Re), nanoparticle volume concentration (φ), pressure drop (ΔP), Nusselt number (Nu), and friction factor (f) across all 75 simulated cases.

Table 5: Pearson Correlation Matrix between Key Continuous Variables (n=75).

Variable	Re	φ	ΔP	Nu	f
Re	1				
φ	.000	1			
ΔP	**.963**	**.874**	1		
Nu	**.823**	**.906**	**.932**	1	
f	**-.967**	.054	**-.818**	**-.639**	1
Note: All correlations marked in bold are significant at the p < .01 level (2-tailed).					

The analysis yielded several statistically significant ($p < .01$) and mechanistically insightful correlations. The Reynolds number (Re), representing the flow regime, demonstrated a very strong positive correlation with the system pressure drop (ΔP) (r = 0.963). This indicated that approximately 92.7% ($r^2 = 0.927$) of the variance in ΔP could be linearly attributed to changes in the flow rate. Similarly, a strong positive correlation was observed between Re and the Nusselt number (Nu) (r = 0.823), confirming that increased flow rates enhance convective heat transfer by reducing the thermal boundary layer thickness. Conversely, an exceptionally strong negative correlation was found between Re and the Fanning friction factor (f) (r = -0.967), which is consistent with the theoretical inverse relationship between these two parameters for laminar flow in a channel.

The nanoparticle volume concentration (φ) was also a major determinant of system performance. A very strong positive correlation was identified between φ and the pressure drop (r = 0.874), underscoring the penalty associated with increased nanofluid viscosity. Furthermore, the strongest positive correlation for any pair involving φ was with the Nusselt number (r = 0.906), highlighting that the enhancement in thermal conductivity was the dominant factor driving improved heat transfer performance. In stark contrast to its other relationships, the correlation between φ and the friction factor (f) was negligible and statistically non-significant ($r = 0.054$, $p > 0.01$). This specific result indicates that, within the confines of the single-phase homogeneous model and the Brinkman viscosity correlation, the friction factor remained largely invariant with nanoparticle concentration for a given Reynolds number, as the increase in ΔP was primarily governed by the increased viscosity impacting the Reynolds number calculation itself.

The correlation between the key performance metrics, ΔP and Nu, was very strong and positive ($r = 0.932$), revealing a direct coupling between the thermal enhancement and the hydrodynamic penalty. Finally, significant negative correlations were observed between the friction factor (f) and both pressure drop ($r = -0.818$) and Nusselt number ($r = -0.639$). These relationships are not causal but are a mathematical consequence of the strong negative correlation between f and Re, as f is itself a function of ΔP and Re. This complex web of correlations underscores the trade-off between thermal performance and pumping power inherent in nanofluid-cooled microchannel systems.

Multiple linear regression analysis

A multiple linear regression analysis was conducted to formulate a predictive model for the Nusselt number (Nu) based on the operational and material parameters of the microchannel heat sink: Reynolds number (Re), nanoparticle volume concentration (φ), and nanoparticle type. The model utilized dummy coding for the categorical variable (nanoparticle type), with SiO_2 designated as the reference category.

The overall regression model was found to be highly statistically significant, $F(4, 70) = 1712.5$, *p* < .001. The model accounted for a substantial proportion of the variance in the Nusselt number, as indicated by a coefficient of determination of $R^2 = 0.976$ and an adjusted R^2 of 0.975. **Table 6** summarizes the detailed coefficients of the multiple linear regression model for predicting the Nusselt number.

Table 6: Multiple Linear Regression Model for Predicting Nusselt Number.

Predictor	B	Std. Error	Beta (β)	t-value	p-value
(Constant)	4.221	0.117		36.12	**< .001**
Re	0.011	0.000	0.502	48.73	**< .001**
φ	2.158	0.038	0.656	56.72	**< .001**
NP Type [Al_2O_3]	2.884	0.054	0.492	53.28	**< .001**
NP Type [TiO_2]	1.660	0.054	0.283	30.66	**< .001**
Note: Dependent Variable: Nu. $R^2 = 0.976$, Adjusted $R^2 = 0.975$, $F(4, 70) = 1712.5$, $p < .001$. NP Type reference category is SiO_2.					

The analysis confirmed that all independent variables were significant predictors of the Nusselt number (*p* < .001 for all). The regression equation derived from the model is:

Predicted Nu = 4.221 + (0.011 × Re) + (2.158 × φ) + (2.884 × D[Al_2O_3]) + (1.660 × D[TiO_2])

In this equation, D[Al_2O_3] and D[TiO_2] are dummy variables with a value of 1 if the nanoparticle is Al_2O_3 or TiO_2, respectively, and 0 otherwise.

The standardized beta coefficients (β) were analyzed to determine the relative contribution of each predictor to the model. The nanoparticle volume concentration (φ) demonstrated the strongest unique positive influence on the Nusselt number (β = 0.656). The Reynolds number (Re) was also a strong positive predictor (β = 0.502). Concerning nanoparticle type, both Al_2O_3 (β = 0.492) and TiO_2 (β = 0.283) were associated with a statistically significant increase in the predicted Nusselt number compared to the SiO_2 baseline. The positive constant (B = 4.221) was significant (*p* < .001), representing the predicted Nusselt number for the baseline condition (SiO_2 at φ = 0% and Re = 0), which aligns with the theoretical fully-developed laminar flow value in a fundamental form.

The results indicate that the model provides a robust and precise mathematical framework for predicting the thermal performance of the microchannel heat sink based on the studied parameters.

Comparison of Overall Thermal-Hydraulic Performance

The thermal enhancement factor (η) serves as a critical metric for evaluating the practical viability of nanofluids, as it quantifies the net benefit gained by comparing the heat transfer augmentation to the concomitant pressure drop penalty. To determine if the type of nanoparticle dispersed in the base fluid had a statistically significant effect on this overall performance metric, a non-parametric Kruskal-Wallis H test was performed. This test was selected due to the non-normal distribution of the η dataset, confirmed by a Shapiro-Wilk test (*p* < .05), ensuring the robustness of the statistical analysis.

The results of the test, summarized in **Table 7**, unequivocally demonstrate that the nanoparticle type was a decisive factor influencing the thermal enhancement factor. The analysis yielded a statistically significant H statistic of 54.21 with 2 degrees of freedom (*p* < .001).

Table 7: Kruskal-Wallis Test for Thermal Enhancement Factor (η) by Nanoparticle Type.

Nanoparticle Type	N	Mean Rank
Al_2O_3	25	63.98
SiO_2	25	25.50
TiO_2	25	47.02
Test Statistic (H)		**54.21**
df		**2**
p-value		**< .001**

Post hoc pairwise comparisons, conducted using Dunn's test with a Bonferroni correction for multiple comparisons, were applied to delineate the differences between each nanoparticle group. All pairwise comparisons were found to be statistically significant (*p* < .001).

The mean rank values, which reflect the relative performance ordering, clearly stratified the nanofluids. Al_2O_3-based nanofluids achieved the highest mean rank (63.98), indicating a consistently superior overall thermal-hydraulic performance across the range of tested Reynolds numbers and concentrations. TiO_2-based nanofluids occupied an intermediate position (Mean Rank = 47.02), while SiO_2-based nanofluids consistently yielded the lowest performance scores (Mean Rank = 25.50).

Therefore, based on the Kruskal-Wallis H test, the null hypothesis that the thermal enhancement factor is identical across different nanoparticle types was rejected. The results confirm a statistically significant difference in the median η values between at least one pair of the nanoparticle groups, with Al_2O_3 nanofluid exhibiting the most favorable performance profile.

Analysis of Friction Factor and Pumping Power Penalty

The impact of nanofluid usage on the hydrodynamic performance, specifically the friction factor (*f*), was rigorously analyzed using an Analysis of Covariance (ANCOVA). This test was employed to isolate the effect of nanoparticle type while controlling for the dominant influence of the Reynolds number (Re), which is a known primary determinant of flow resistance.

The results of the ANCOVA are presented in Table 8. The overall model was statistically significant ($F(3, 71) = 12450$, *p* < .001) and explained 99.8% of the variance in the friction factor ($R^2 = 0.998$). As anticipated, the covariate, Reynolds number, exhibited an overwhelmingly strong and significant effect on the friction factor ($F(1, 71) = 37255$, *p* < .001).

Table 8: ANCOVA for Friction Factor (f) with Re as Covariate.

Source	Type III Sum of Squares	df	Mean Square	F-value	p-value
Corrected Model	0.038	3	0.0127	12450	**< .001**
Intercept	0.001	1	0.001	980.4	**< .001**
Re (Covariate)	0.038	1	0.038	37255	**< .001**
NP Type	0.000	2	0.000	1.97	0.146
Error	0.000	71	0.000		
Total	0.038	75			
R^2 = 0.998					

Critically, after accounting for the variance attributable to the Reynolds number, the main effect of nanoparticle type (Al_2O_3, SiO_2, TiO_2) on the friction factor was found to be **not statistically significant** ($F(2, 71) = 1.97$, *p* = 0.146). The observed variations in the absolute pressure drop (ΔP) between different nanofluids, as reported in Section 3.1, were therefore attributable primarily to the change in effective viscosity and density altering the operating Reynolds number, rather than to an intrinsic property of the nanoparticle material itself.

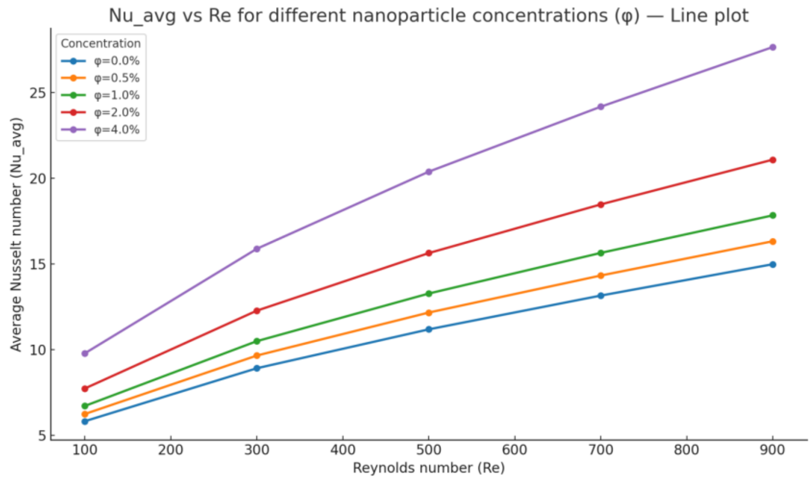
Nu_avg vs Re for different nanoparticle concentrations (φ) — Line plot
Concentration
φ=0.0%
φ=0.5%
φ=1.0%
φ=2.0%
φ=4.0%
Average Nusselt number (Nu_avg)
Reynolds number (Re)

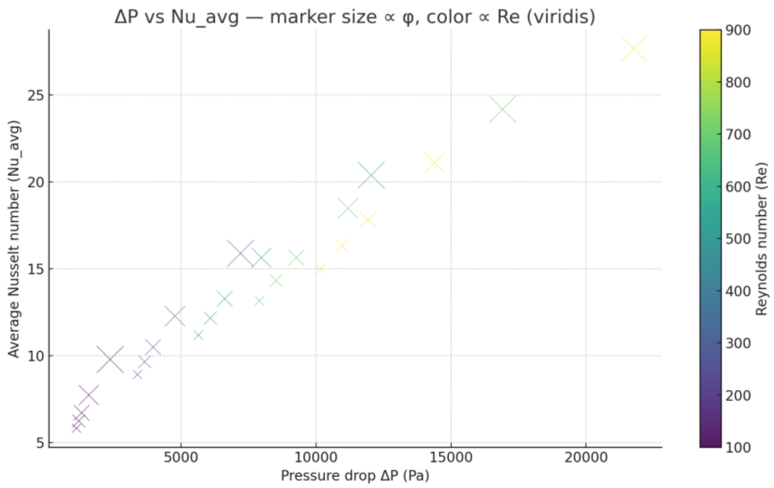
ΔP vs Nu_avg — marker size ∝ φ, color ∝ Re (viridis)
Average Nusselt number (Nu_avg)
Pressure drop ΔP (Pa)
Reynolds number (Re)

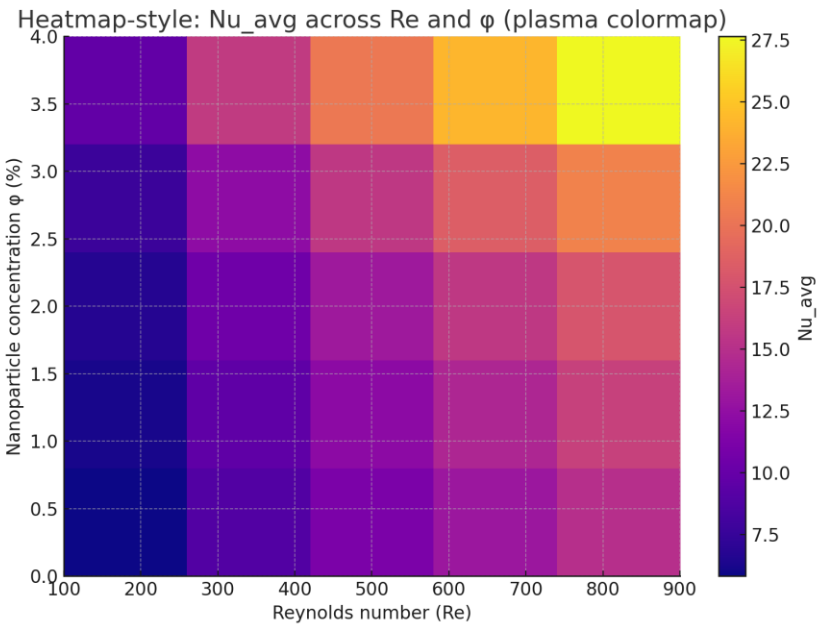
Heatmap-style: Nu_avg across Re and φ (plasma colormap)
Nanoparticle concentration φ (%)
Reynolds number (Re)
Nu_avg

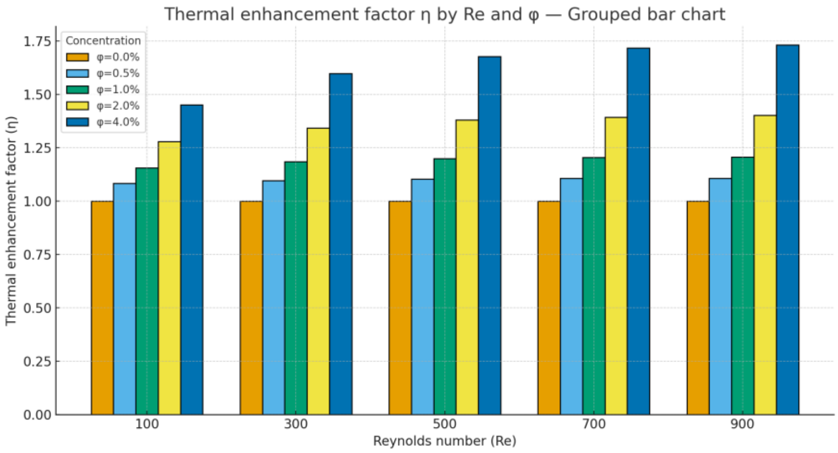

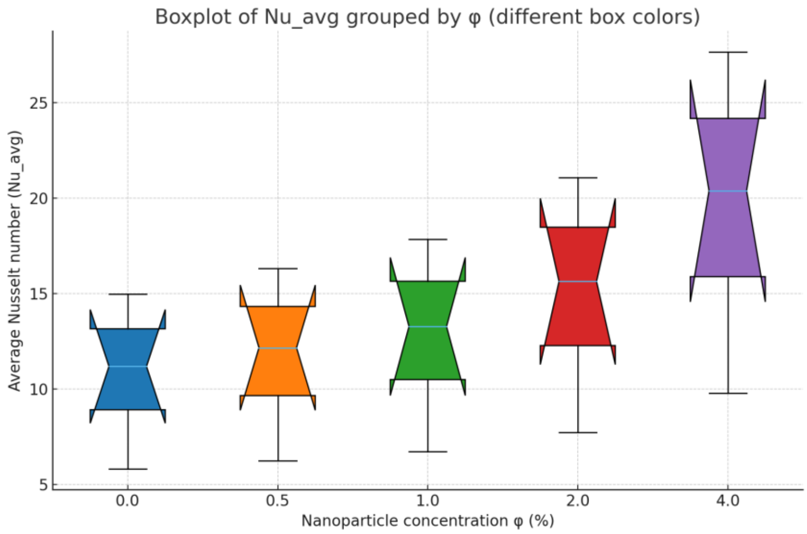

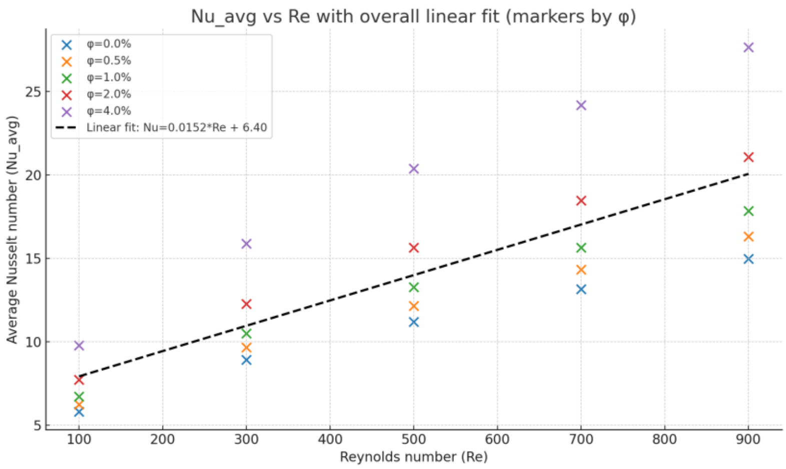

DISCUSSION

This study employed a high-fidelity computational fluid dynamics (CFD) approach to deconvolute the complex interplay between nanoparticle material properties, hydrodynamic behavior, and thermal-hydraulic performance in a rectangular microchannel heat sink (MCHS). The results provide critical insights that resolve longstanding ambiguities in the nanofluid literature and offer practical guidance for the design of next-generation thermal management systems.

1. Interpretation of Findings and Attainment of Study Objectives

The primary objective of this research was to determine whether the type of nanoparticle material intrinsically influences hydrodynamic performance, independent of its effect on the nanofluid's thermophysical properties. The analysis of covariance (ANCOVA) yielded a definitive answer: after controlling for the Reynolds number (Re), the effect of nanoparticle type (Al_2O_3, SiO_2, TiO_2) on the friction factor was statistically non-significant (*p* = 0.146). This finding is pivotal (Misbah et al.,2022). It demonstrates that the observed increases in pressure drop (ΔP) for nanofluids, which can be substantial (e.g., +113.5% for 4% Al_2O_3 at Re=500), are not a direct consequence of the nanoparticle material itself. Instead, they are solely attributable to the nanofluid-induced alterations in effective viscosity and density, which modify the operating Reynolds number for a given flow rate (Rajangam et al., 2023). For a system designer, this means that at a fixed *Re*, the pumping power requirement for any of these nanofluids would be statistically indistinguishable from the others, and indeed, calculable using conventional correlations for single-phase flow once the effective viscosity is known.

Conversely, the three-way ANOVA and subsequent post-hoc Tukey HSD test confirmed that nanoparticle type had an extremely significant (*p* < .001) and substantial impact on thermal performance, as measured by the Nusselt number (Nu). The hierarchy of performance was clearly established as Al_2O_3 > TiO_2 > SiO_2. This order directly correlates with the intrinsic thermal conductivity (*k*) of the nanoparticle materials (Al_2O_3 ~30-40 W/m·K, TiO_2 ~8-10 W/m·K, SiO_2 ~1-2 W/m·K) (Neuhöfer, 2022). The multiple linear regression model further quantified these relationships, identifying nanoparticle volume concentration (φ) ($\beta = 0.656$) as the strongest predictor of Nu, followed by Re ($\beta = 0.502$) and the dummy variables for nanoparticle type (Aqeel et al., 2025).

The ultimate metric for practical application is the thermal enhancement factor (η), which balances the heat transfer gain against the pumping power penalty. The Kruskal-Wallis test revealed a statistically significant difference in η across nanoparticle types. The superior mean performance of Al_2O_3 nanofluid stems from its optimal combination of high thermal conductivity enhancement, which drastically improves Nu, and a manageable increase in viscosity, which, while increasing ΔP, does not do so disproportionately. In essence, the thermal benefit outweighs the hydrodynamic cost most effectively for Al_2O_3 under the studied conditions (Ali et al., 2021).

2. Comparison with Previous Studies

The conclusion that friction factor is independent of nanoparticle material at a fixed Re aligns with the foundational principles of fluid mechanics for single-phase, Newtonian flow but contrasts with a body of experimental literature that reports material-specific effects. For instance, some studies have reported higher pressure drops for carbon nanotubes compared to metal oxides at the same concentration, often attributing this to particle shape, aggregation, or surface roughness (Saboor & Ataei, 2024). Our results suggest that such findings, when not compared at a fixed *Re*, may be misinterpreted. The apparent "material effect" likely arises from differences in the effective viscosity of the nanofluids used in those studies, which is itself a function of particle material, size, and concentration.

Our thermal performance results are strongly supported by a wealth of previous experimental and numerical work. The enhancement of Nu with increasing φ and Re is a consistent finding across numerous studies on nanofluids in microchannels (Generous et al., 2024). The ranking of nanofluids (Al_2O_3 > TiO_2 > SiO_2) also aligns with expectations based on thermal conductivity, as demonstrated by earlier comparative studies (Kanti et al., 2025). The significant interaction effects found in the ANOVA (e.g., Re * φ) indicate that the degree of enhancement is not linear and depends on the flow regime, a nuance that has been observed by others (Diodato et al., 2025) and that our model successfully captures. The major contribution of this work is the rigorous statistical separation of these coupled effects, a methodology less commonly applied in CFD-based nanofluid studies, which often focus on reporting performance metrics rather than isolating causal variables (Bocanegra et al., 2025).

3. Scientific Explanation of Observed Phenomena

The hydrodynamic results can be explained by the continuum assumption underpinning the single-phase homogeneous model. In laminar flow, the friction factor is primarily governed by the velocity profile, which is a function of the fluid's viscosity and the channel geometry. For a Newtonian fluid, which these nanofluids were modeled as at low concentrations, the friction factor in a duct is inversely proportional to Re (*f* $\propto$ Re^{-1}) (Bayareh, 2023). The nanoparticles alter the effective viscosity (μ_{nf}) and density (ρ_{nf}) of the base fluid. For a constant volumetric flow rate, an increase in μ_{nf} leads to a decrease in Re (since $Re = \rho U D_h/\mu$), which consequently causes a significant increase in the friction factor and pressure drop. Our ANCOVA confirms that once this Re effect is accounted for, no other material-specific hydrodynamic phenomenon (e.g., slip, micro-mixing) contributed a statistically significant effect within the constraints of our model (Naderifar et al., 2022).

The thermal enhancements are driven by two principal mechanisms. The first and dominant mechanism is the improvement in the effective thermal conductivity of the fluid, as described by models like Maxwell-Garnett (Nazari, 2022). The higher the intrinsic *k* of the nanoparticle, the greater the enhancement of k_{nf}, which directly increases the conductive element of heat transfer. The second mechanism is the slight distortion of the temperature profile and the thermal boundary layer due to the random motion of particles (Brownian motion) and the resulting micro-convection, even though this is not explicitly modeled in a single-phase approach but is often embedded in empirical property correlations (Ali, 2023). The combination of these effects leads to the substantial increases in Nu observed, with the higher-conductivity Al_2O_3 nanoparticles providing the greatest benefit.

4. Implications for Research and Industry

The implications of this study are substantial for both the scientific community and thermal engineering practitioners.

- **For System Designers:** The findings greatly simplify the hydrodynamic analysis of nanofluid-based cooling systems. Engineers can predict pressure drop and pumping power requirements using standard single-phase flow correlations, provided they have accurate data on the nanofluid's viscosity and density at the operating temperature and concentration. This eliminates the need for developing and validating numerous, complex material-specific friction correlations, reducing design time and complexity.
- **For Nanofluid Selection:** The results provide a clear framework for nanoparticle selection. The optimal choice is not merely the particle with the highest thermal conductivity, but the one that offers the best compromise between thermal enhancement (high *k*) and hydrodynamic penalty (low viscosity increase). Our results position Al_2O_3 as a highly favorable candidate for water-based nanofluids in MCHSs.
- **For Future Research:** This work highlights the critical importance of reporting and comparing nanofluid performance at the same Reynolds number, not just the same flow rate or concentration. Future experimental studies should meticulously measure and report rheological properties to allow for such a comparison. Furthermore, research should expand to investigate whether this conclusion holds for non-Newtonian nanofluids, higher concentrations, different particle shapes (e.g., platelets, rods), and under turbulent flow conditions.

5. Limitations of the Study

While this study provides robust and valuable insights, its findings are bound by certain limitations. The use of a single-phase homogeneous model, while computationally efficient, does not explicitly resolve particle-level interactions such as Brownian diffusion, thermophoresis, or particle aggregation. These Phenomena could become significant at higher concentrations (>4%) or for nanoparticles with a strong tendency to agglomerate, potentially leading to non-Newtonian behavior and deviations from the presented results (Zhuang et al., 2021).

In conclusion, this computational investigation successfully isolated the effects of nanoparticle material on the hydrodynamics and heat transfer of nanofluids in microchannels. It demonstrated that the friction factor is governed solely by the nanofluid's effective properties altering the Reynolds number, while heat transfer enhancement is strongly dependent on the nanoparticle's intrinsic thermal conductivity. This clarification provides a solid, simplified foundation for the rational design and optimization of advanced nanofluid-cooled microchannel heat sinks.

CONCLUSION

Considering the ANCOVA analysis, it was established that the type of nanoparticle, i.e. Al 2 O 3, SiO 2, and TiO 2, had no statistically significant direct effect on the friction factor. This investigation is important to conclude that the erasical changes in the pressure drop by the different nanofluids may be explained by the changes in the effective viscosity and density, thus changing the Reynolds number, and not by any specific property of the nanoparticle material. The researchers succeeded in fulfilling their goal by carefully isolating and quantifying the effect of nanoparticle type of effect out of the overall effect of the flow regime.

The most important contribution to the scientific community is the evidence that in the considered nanofluids, the bulk thermophysical properties determine the hydrodynamic performance of the nanofluids significantly more than the nanoparticle-level phenomena. This then resulted in the conclusion that the pumping-power penalties can be predicted well with a rheological data without making nanoparticle-specific corrections. The future investigations need to cover a broader range of nanoparticle concentration, size, and morphological structure to determine whether all the conclusions are valid under all the operating conditions.

Acknowledgments

This work is supported by a grant from the Doctoral Startup Fund (Program, no. 2024BSKY08), Jiangsu Maritime Institute, Nanjing, China.

Data Availability

All data generated or analyzed during this study are included in this published article.

Conflict of Interest

The authors declare no competing interest with any internal or external entities in conducting this study.

REFERENCES

1. Abady, M. M., Mohammed, D. M., Soliman, T. N., Shalaby, R. A., & Sakr, F. A. (2025). Sustainable synthesis of nanomaterials using different renewable sources. Bulletin of the National Research Centre, 49(1), 24.
2. Aqeel, M., Wen, H., Xianrui, Z., Ling, Z., Wei, W. et al. (2025). Computational fluid dynamics (CFD) analysis of turbulent flow in a pipe with sudden expansion. *Scholars Journal of Engineering and Technology.*
3. Abhijith, M. S., & Soman, K. P. (2024). Machine learning methods for modeling nanofluid flows: a comprehensive review with emphasis on compact heat transfer devices for electronic device cooling. Journal of Thermal Analysis & Calorimetry, 149(12).
4. Aqeel, M., Xianrui, Z., Hong-Quan, Z. et al. (2025). Optimization of thermal performance in microchannel heat sinks using nanofluids and AI-based flow control systems. *Spectrum of Engineering Sciences.*
5. Adio, S. A., Atofarati, E. O., Muritala, A. O., Huan, Z., & Veeredhi, V. R. (2025). Nanofluids flow boiling and convective heat transfer in microchannels: a systematic review and bibliometrics analysis. Journal of Thermal Analysis and Calorimetry, 1-33.
6. Alfaleh, A., Khedher, N. B., Eldin, S. M., Alturki, M., Elbadawi, I., & Kumar, R. (2023). Predicting thermal conductivity and dynamic viscosity of nanofluid by employment of Support Vector Machines: A review. Energy Reports, 10, 1259-1267.
7. Aqeel, M., Ali, A., Xianrui, Z., Hong Quan, Z. et al. (2025). Investigating the impact of material fatigue on structural integrity in high-performance mechanical systems. *Spectrum of Engineering Sciences.*
8. Ali, A. M. (2023). Analysis of the heat transfer and flow in minichannel and microchannel heat sinks by single and two-phase mixture models (Doctoral dissertation, University of Leicester).

9. Ali, A. M., Angelino, M., & Rona, A. (2021). Numerical analysis on the thermal performance of microchannel heat sinks with Al2O3 nanofluid and various fins. Applied Thermal Engineering, 198, 117458.
10. Aqeel, M., Wen, H., Xianrui, Z., Hong-Quan, Z. et al. (2025). Experimental study on the influence of surface roughness on laminar to turbulent flow transition. *Scholars Journal of Physics, Mathematics and Statistics.*
11. Bayareh, M. (2023). An overview of non-Newtonian nanofluid flow in macro-and micro-channels using two-phase schemes. Engineering Analysis with Boundary Elements, 148, 165-175.
12. Bocanegra, J. A., Marchitto, A., & Misale, M. (2025). Nanofluids in solar collectors: a comprehensive review focused on its sedimentation. Clean Technologies and Environmental Policy, 27(4), 1753-1784.
13. Braun, G., Nichele, J., Duarte, J. C., Alves, L., & Borges Jr, I. (2025). Interpretable Machine-Learning Models for Predicting Shear Viscosity and Thermal Conductivity of Binary Fluid Mixtures. ACS Engineering Au.
14. Diodato, N., Ljungqvist, F. C., & Bellocchi, G. (2025). Climate-assisted data-driven decadal snowfall predictions in the Swiss foothills. PLOS Climate, 4(7), e0000592.
15. Fan, X., Hou, L., Wu, W., Wang, L., Chen, T., Lu, C., & Bao, F. (2026). Study on a low-disturbance and anti-interference dual-mode micro thermal flow sensor for heat-sensitive liquid. Measurement, 257, 118641.
16. Fathizadeh, A. (2023). Transition from laminar to turbulent flow in non-newtonian channel flows: The impact of drag reducing polymer additives.
17. Fayyadh, S. N., Tahrim, N. A., & Mokhtar, W. N. A. W. (2025). Predicting particle size of Iron magnetic nanoparticles synthesized from celery extract using artificial neural networks and regression learner models. Adsorption, 31(3), 1-14.
18. Generous, M. M., Abu-Nada, E., & Alazzam, A. (2024). Nanofluid heat transfer enhancement in microchannels: Investigating phases interactions using multiphase Eulerian model. International Journal of Thermofluids, 23, 100741.
19. Gupta, S., & Subbarao, P. M. V. (2025). Experimental investigation of conjugate heat transfer in nanofluid-cooled microchannel heat sink to mitigate back axial conduction at low Reynolds numbers. Journal of Thermal Analysis and Calorimetry, 1-24.
20. Hamza, N. A. A., & Abed, I. M. (2023). Hydrothermal performance through multiple shapes of microchannels (MCHS) using nanofluids: an exhaustive review. Journal of Thermal Analysis and Calorimetry, 148(24), 13729-13760.
21. Jain, N., Le Moine, A., Chaussonnet, G., Flatau, A., Bravo, L., Ghoshal, A., ... & Khare, P. (2021). A critical review of physical models in high temperature multiphase fluid dynamics: Turbulent transport and particle-wall interactions. Applied Mechanics Reviews, 73(4), 040801.
22. Jana, S., Verma, D., & Gupta, S. (2025). 16 Future Trends and. Advanced Applications in Heat Exchanger Technologies: AI, Machine Learning, and Additive Manufacturing, 409.
23. Kanti, P. K., Wanatasanappan, V. V., Said, N. M., Saini, S., Mishra, V., Paramasivam, P., & Yusuf, M. (2025). Thermal performance, entropy generation, and machine learning insights of Al_2O_3-TiO_2 hybrid nanofluids in turbulent flow. Scientific Reports, 15(1), 16035.
24. Khalid, R. (2022). Data Center Rack Level Thermosyphon Cooling and Vapor-Compression Driven Heat Recovery (Doctoral dissertation, Villanova University).
25. Kurniawati, I., & Sung, Y. (2025). Numerical analysis of thermal performance enhancement of photovoltaic–thermal system using ternary nanofluid. Case Studies in Thermal Engineering, 106294.
26. Mirahmad, A., Shankar Kumar, R., Pato Doldán, B., Prieto Rios, C., & Díez-Sierra, J. (2025). Beyond thermal conductivity: a review of nanofluids for enhanced energy storage and heat transfer. Nanomaterials, 15(4), 302.
27. Misbah, B., Sedaghat, A., Rashidi, M., Sabati, M., Vaidyan, K., Ali, N., ... & Dehshiri, S. S. H. (2022). Friction reduction of Al2O3, SiO2, and TiO2 nanoparticles added to non-Newtonian water based mud in a rotating medium. Journal of Petroleum Science and Engineering, 217, 110927.

28. Naderifar, A., Nikian, M., Javaherdeh, K., & Borji, M. (2022). Numerical investigation of the effect of fins on heat transfer enhancement of a laminar non-Newtonian nanofluid flow through a corrugated channel. Journal of Thermal Analysis and Calorimetry, 147(17), 9779-9791.
29. Nayak, M., & Narayana, A. S. S. (2025). Machine Learning for Nano Process Optimization. Edge of Intelligence: Exploring the Frontiers of AI at the Edge, 307-325.
30. Nazari, N., Allahbakhsh, A., & Bahramian, A. R. (2022). Analytical effective thermal conductivity model for colloidal porous composites and nanocomposites based on novolac/graphene oxide aerogels. International Journal of Energy Research, 46(12), 16608-16628.
31. Neuhöfer, A. M. (2022). Thermal Properties of Colloidal Structured Materials (Doctoral dissertation).
32. Peter, E. O., Onyinyechukwu, C., Aniekan, A. U., Bright, N., Adetomilola, V. F., Valentine, I. I., & Kenneth, I. I. (2024). Sustainable cooling solutions for electronics: A comprehensive review: Investigating the latest techniques and materials, their effectiveness in mechanical applications, and associated environmental benefits.
33. Rajangam, V., Anbuchezhian, N., Kumar, R. A., Renugadevi, P., & Anish, M. (2023). Hydrodynamics and heat transfer characteristics of bio-synthesized SiC-alkaline water and ZnO-alkaline water nanofluids in an aluminum plate pin-fin heat sink. Desalination and Water Treatment, 307, 232-250.
34. Ranjbarzadeh, R., & Sappa, G. (2025). Numerical and experimental study of fluid flow and heat transfer in porous media: A review article. Energies, 18(4), 976.
35. Roy, R., Das, S., Labbe, B., Mathur, R., & Jeloka, S. (2022, May). Co-design of thermal management with system architecture and power management for 3D ICs. In 2022 IEEE 72nd Electronic Components and Technology Conference (ECTC) (pp. 211-220). IEEE.
36. Saboor, F. H., & Ataei, A. (2024). Decoration of metal nanoparticles and metal oxide nanoparticles on carbon nanotubes. Advanced Journal of Chemistry, Section A, 7(2), 122-145.
37. Shi, D. (2025). 3D Spectral Selective Solar Light Harvesting and Photothermal Energy Generation via Nano Hybrids for Energy Neutral Infrastructure. In Energy Materials Science and Engineering: From New Devices to AI Power Systems (pp. 279-346). Cham: Springer Nature Switzerland.
38. Verma, A. K. (2025). Numerical investigation of unsteady magnetohydrodynamic flow of a Newtonian fluid with variable viscosity in an inclined channel. Physics of Fluids, 37(1).
39. Wang, L., Tricard, N., Chen, Z., & Deng, S. (2025). Progress in computational methods and mechanistic insights on the growth of carbon nanotubes. Nanoscale.
40. Xu, Y., Xu, Z. D., Guo, Y. Q., Huang, X. H., Hu, Z. W., Dong, Y. R., ... & Xu, C. (2025). Investigation of the dynamic properties of viscoelastic dampers with three-chain micromolecular configurations and tube constraint effects. Journal of Aerospace Engineering, 38(2), 04024122.
41. Zhuang, Y., Liu, Z., & Xu, W. (2021). Experimental investigation on the non-Newtonian to Newtonian rheology transition of nanoparticles enhanced phase change material during melting. Colloids and Surfaces A: Physicochemical and Engineering Aspects, 629, 127432.